

## Coherent Ladar Angle Estimation Error Analysis

Dr. Philip Gatt and Dr. Scott Shald

Lockheed Martin Coherent Technologies

135 South Taylor Ave. Louisville, CO 80027, [phil.gatt@lmco.com](mailto:phil.gatt@lmco.com)

### INTRODUCTION

Multipixel coherent receivers are not yet commonplace. However, these types of receivers are gaining popularity and it is important to understand their measurement limits. In particular, the angle estimates (from a centroiding technique) produced by a coherent array are intimately tied to the LO pattern on the receiver. This work examines the angle estimation error from one example arrangement. This theory is then shown to compare favorably to Monte Carlo simulation results.

### COHERENT LADAR DESCRIPTION

This following analysis assumes the ladar receiver contains a quad-cell detector in the focal plane illuminated by a Gaussian LO that is centered on the quad-cell. Likewise the transmit beam is Gaussian with  $\exp(-2)$  irradiance radius  $\omega$ , in the aperture-plane.

A key ladar performance metric is the mean carrier-to-noise ratio, *CNR*. The short-pulse diffuse-target *CNR* can be written as<sup>1</sup>

$$CNR = \frac{\eta E_x}{h\nu} T^2 \lambda^2 \iint \rho_\pi I_x I_b dx dy \quad (1)$$

where  $\eta$  is the system efficiency which includes detector quantum efficiency, optics losses, transmit and back-propagated local oscillator (BPLO) truncation, but not heterodyne mixing efficiency. The latter is captured in the overlap integral of the normalized transmit and BPLO beams  $I_x$  and  $I_b$ . These beams are normalized to unit power in the target plane. Also,  $h$  is Planck's constant,  $\nu$  and  $\lambda$  are the optical frequency and wavelength,  $T$  is the one way transmission, and  $\rho_\pi$  is the target reflectance ( $\text{sr}^{-1}$ ).

From Eq 1, it is obvious that for a far-field on-axis point target the *CNR* is maximized when the transmit beam Strehl is maximized. With a circular aperture of radius  $a$ , this is achieved when the beam truncation ratio,  $\rho_x = \omega/a$ , is  $89.21\%^2$ . The local oscillator configuration which maximizes the BPLO on-axis irradiance and the point-target *CNR* is one that is matched to the transmit beam but is

pre-truncated before illuminating the detector such that no excess LO power is on the detector.

### ANGLE ERROR-SIGNAL VARIANCE

The azimuth (or elevation) error-signal is derived from the two composite photocurrents representing bi-cell detector elements (i.e., the sum of lower and upper quad-cell currents). Each bi-cell current is modeled as

$$r_i = s_i + n_i \quad (2)$$

Here  $r_i$  is the noise-corrupted heterodyne signal *complex amplitude* in the  $i^{\text{th}}$  bi-cell channel;  $s_i$  is the *speckle modulated signal complex amplitude*; and  $n_i$  is additive narrowband circular complex Gaussian noise, representing local oscillator shot-noise.

The angle error-signals are derived from bi-cell signal power estimates. For example, the azimuth error-signal is derived from

$$\varepsilon = (\hat{P}_{s1} - \hat{P}_{s2}) / (\hat{P}_{s1} + \hat{P}_{s2}), \quad (3)$$

where  $\hat{P}_{si}$  are signal power estimates derived by estimating the total power,  $\hat{P}_i$ , and subtracting the noise power estimate  $\hat{P}_{ni}$ . If we assume the signals are normalized such that the mean noise power is 1, then

$$\hat{P}_{si} = \hat{P}_i - 1 = \sum_M |r_j|^2 / M - 1. \quad (4)$$

The power estimate means are given by

$$E[\hat{P}_{si}] = CNR_i \quad \text{and} \quad E[\hat{P}_i] = CNR_i + 1 \quad (5)$$

For a diffuse target and vacuum speckle, the distribution of the total power estimates,  $\hat{P}_i$ , is known to follow a gamma distribution. Therefore the variance equals the square-mean divided by the diversity or number of independent measurements averaged,  $M$ . This leads to

$$\text{var}[\hat{P}_{si}] = \text{var}[\hat{P}_i] = (CNR_i + 1)^2 / M. \quad (6)$$

These results concur with Shapiro's "Image"  $SNR^3$ , for vacuum or free-space speckle. That is,

$$SNR_i = E[\hat{P}_{si}]^2 / \text{var}[\hat{P}_{si}] = M CNR_i^2 / (CNR_i + 1)^2. \quad (7)$$

Using perturbation theory, it can be shown that the variance of the error-signal is given by

$$\text{var}[\varepsilon] = \left( \frac{2E[\hat{P}_{s1}]E[\hat{P}_{s2}]}{(E[\hat{P}_{s1}] + E[\hat{P}_{s2}])^2} \right)^2 \left( \frac{1}{SNR_1} + \frac{1}{SNR_2} - \frac{2\gamma_{\hat{P}_s}}{\sqrt{SNR_1 SNR_2}} \right), \quad (8)$$

where  $\gamma_{\hat{P}_s}$  is the power estimate correlation coefficient. Hence, even with low  $SNR$ , the error-signal variance can be very small if the signals have nearly equal strength and are highly correlated.

### ANGLE ESTIMATE VARIANCE

To first order, the angle estimate variance of any general angle sensor is given by<sup>4</sup>

$$\text{var}[\theta] \approx \Delta\theta^2 / SNR, \quad (9)$$

where  $\Delta\theta$  is the angular resolution and  $SNR$  is the signal-to-noise ratio.

For the quad-cell arrangement described above, the discriminator function is quasi-linear and the angle estimate is given by  $\theta = \varepsilon/\beta$ , where

$$\beta = \partial\varepsilon/\partial\theta, \quad (10)$$

is the discriminator slope or sensitivity. Thus, the angle variance scales with the error-signal variance derived above. That is,

$$\text{var}[\theta] = \text{var}[\varepsilon]/\beta^2. \quad (11)$$

Thus, finer angular resolution ( $\lambda/D$ ) results in increased  $\beta$  and less angle error.

In this paper, we show that for a diffraction limited receiver  $\beta \approx D/\lambda$ . This is because the error-signal is expected to have a full range of  $\pm 1$  over an angle on the order of  $\pm \lambda/D$ . The exact value of  $\beta$  will depend upon the target-plane beams (transmit, and two BPLO beams) and on the target shape and reflectivity.

Consider the special case of an on-axis point target where  $CNR_1 \approx CNR_2$ . Further assume,  $\gamma_{\hat{P}_s} \approx 0$ , due to, for example, low  $CNR$ . In this case the angle error variance becomes

$$\text{var}[\theta] = 1/2\beta^2 SNR. \quad (12)$$

This agrees with the first order estimate provided in Eq. 9 with an angular resolution,  $\Delta\theta \approx 1/\sqrt{2}\beta$ .

Now consider the same conditions but with  $\gamma_{\hat{P}_s} \approx 1$ . Here the angle error variance is nearly zero, since the speckle noise is highly correlated and the two signals fluctuate nearly identically. Therefore, a critical component to the noise analysis is the power estimate degree of correlation.

### POWER ESTIMATE CORRELATION

The power estimate correlation coefficient depends on both the strength of the two signals and the relative overlap of the bi-cell BPLO beams on the target. It is straight forward to show that the covariance of the power estimates is equal to the covariance of the noise free signal powers. The latter includes speckle noise but not LO shot noise.

$$C_{\hat{P}_s} = C_{P_s} \quad \text{or} \quad \gamma_{\hat{P}_s} \sigma_{\hat{P}_{s1}} \sigma_{\hat{P}_{s2}} = \gamma_{P_s} \sigma_{P_{s1}} \sigma_{P_{s2}}, \quad (13)$$

where  $\sigma = \sqrt{\text{var}}$ . Using Eq. 6 and the fact that  $\text{var}[P_s] = E[P_s]^2 = CNR^2$ , leads to

$$\gamma_{\hat{P}_s} = \gamma_{P_s} \frac{CNR_1 CNR_2}{(1 + CNR_1)(1 + CNR_2)}, \quad (14)$$

These expressions are combined to yield the results shown in Fig. 1. This figure shows the error-signal variance as a function of  $CNR$ , for the special case when  $CNR_1 = CNR_2$ . As can be seen, speckle-limited performance is achieved when the  $CNR > \sim 10$  dB, for the weakest of the two bi-cell signals. Under this condition the performance dramatically improves as the speckle-limited correlation coefficient increases.

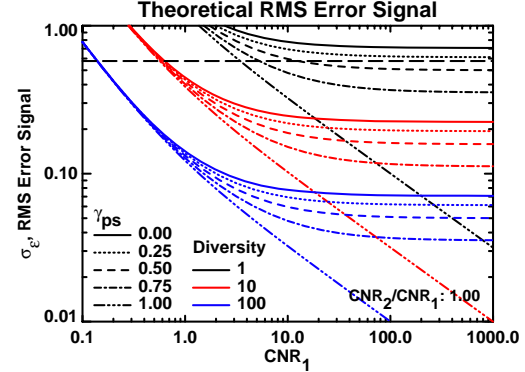


Figure 1 Theoretical RMS error-signal vs  $CNR$  parametric in diversity and the speckle degree of correlation, assuming equal  $CNR$ s.

The remaining question to be answered is how are the two speckle-limited power estimates correlated? The analysis starts with the recognition that the speckle degree of correlation is the square-magnitude of the heterodyne signal correlation.

$$\gamma_{P_s} = |\gamma_s|^2 = \left| \frac{E[s_1 s_2^*]}{E[|s_1|^2] E[|s_2|^2]} \right|^2. \quad (15)$$

The above result follows from the complex Gaussian moment theorem<sup>5</sup>, and is only valid for

zero-mean complex Gaussian random variables. This constraint is satisfied by heterodyne signals with vacuum speckle and additive narrowband noise.

Thus, the problem involves deriving the speckled heterodyne signal degree of correlation,  $\gamma_s$  which requires an expression for the two noiseless photocurrents  $s_1$  and  $s_2$ . It can be shown that in a coherent receiver the photocurrent is proportional to a field overlap integral in the target-plane. That is

$$s_i = \sqrt{\eta E_x T \lambda} \iint a_s(x, y) u_x(x, y) u_b(x, y) dx dy, \quad (16)$$

where  $u_x$  and  $u_b$  are the normalized target-plane transmit and BPLO fields, respectively, and  $a_s$  is the target complex scattering amplitude, such that  $|a_s|^2 = \rho_\pi$ .

By substituting this expression into Eq. 15, reversing the order of integration and expectation, assuming that individual target scattering centers are not resolved by the beam (i.e., the target's surface height autocorrelation function is modeled as a delta function such that a 4<sup>th</sup> order integral can be reduced to a single 2<sup>nd</sup> order integral), and simplifying, produces the following result.

$$\gamma_{p_s} = \frac{\left| \iint \rho_\pi I_x u_{b1} u_{b2}^* dx dy \right|^2}{\iint \rho_\pi I_x I_{b1} dx dy \iint \rho_\pi I_x I_{b2} dx dy}, \quad (17)$$

where  $I = |u|^2$  is the field irradiance, and the subscripts  $x$ ,  $b1$  and  $b2$  represent the transmit and two bi-detector BPLO beams.

Consider if  $u_{b1}$  and  $u_{b2}$  are spatially proportional to each other, then by Schwartz' inequality, the degree of correlation is unity. This applies to a dual-port photoreceiver. Also consider the case of a point target. Here the integrals reduce to the integrand evaluated at the target position. If this point target is on-axis, such that the two BPLO beam irradiances are equal, then the numerator and denominator are equal, producing unit correlation. Finally consider the infinite aperture and focused condition where the  $u_{b1}$  and  $u_{b2}$  are spatially separate. In this case the degree of correlation is zero, since both detectors see different parts of the target and there is no shared target component between the two signals.

## LADAR SIGNAL SIMULATION & RESULTS

A coherent ladar signal simulator was developed to produce simulated heterodyne signal complex amplitudes, using target plane overlap integrals. Stochastic signals were generated via Eq. 16 and mean power estimates were calculated using Eq. 4, for arbitrarily shaped diffuse targets. Example results from an experiment characterizing performance as a function of target position is shown below. As can be seen, the simulation results and the theory corroborate each other.

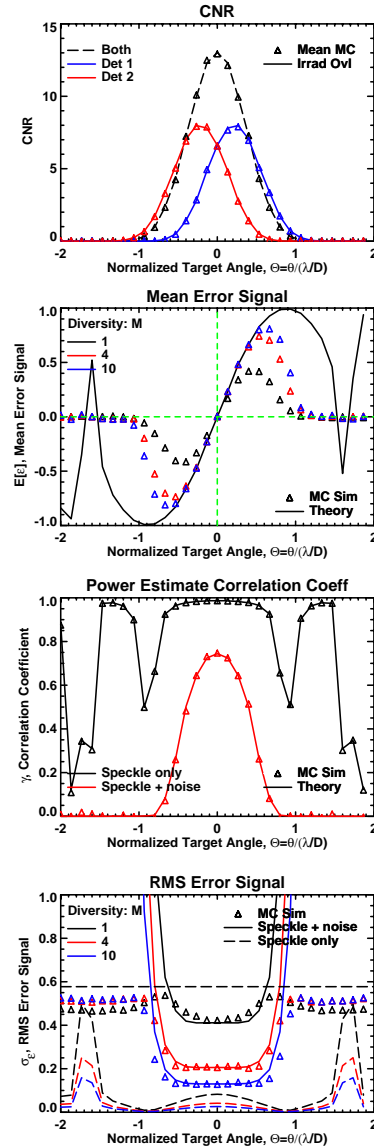


Figure 2 Simulation measured ( $\Delta$ ) and theoretical (solid) results as a function of normalized target far-field angle. The target was an  $\sim 2$  m diameter diffuse disc and the far-field beam spot size was  $\sim 8$  m.

## LADAR TRACK SIMULATOR & RESULTS

A tracking simulation was developed to evaluate the utility of the angle measurements provided by the ladar. In this simulation, the ladar provides range, velocity, and angle/angle measurements (if a detection is declared) to a target tracker (a Kalman filter) that estimates the target's trajectory. Then pointing angles are computed based upon the updated target track and sent to the pointing system. The ladar then interrogates this new pointing direction looking for new target returns. Since this is a closed-loop tracking system, it will only succeed if the angle/angle measurements provided by the ladar are accurate and timely.

Figure 3 shows the results from the tracking simulation. The first result to notice is that the ladar is able to produce thousands of detections of the target in this scheme, which is a good indication that the angle information is useful to the tracker. The measured *CNR* values show speckle effects from this diffuse target and indicate the threshold that was being used (about 4). The raw position error is mainly due to the angle error (since the range error in this case was only a fraction of a meter). The angle measurements improve at the middle of the simulation where *CNR* is maximum.

The filtered position error shows the output of the Kalman filter, and it shows that the filtering (after settling through some transients) is able to reject most of the noise in the raw measurements. In this case, the angle measurements from the ladar (as well as the range and velocity measurements) allow for track accuracy near 1 m. Although the angle measurements are only one part of this tracking simulation, they are a critical part and the results show that they do support closed-loop target tracking.

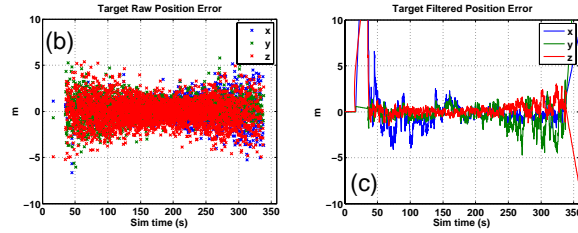
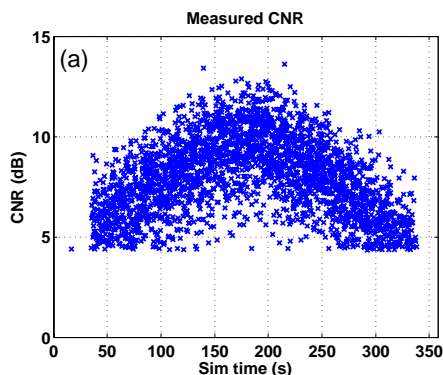


Figure 3 Tracking simulation results: *CNR* (a), raw ladar (b) and filtered ladar (c) position errors. The *CNR* and raw ladar position estimates were derived from 10 independent measurements.

## SUMMARY

In this paper we developed the basic theory governing the performance of angle measurements in a quad-cell based coherent ladar. Performance was shown to depend on many factors. Key factors include the signal *CNR*s, the discriminator slope, which is maximized ( $\beta \approx D/\lambda$ ) for diffraction limited sensors, and the degree of power estimate correlation. The latter depends upon the *CNR*, target size and position, and BPLO configuration. It was shown that angle errors agree with first order models if the two bi-cell power estimates are uncorrelated but that the errors can be much smaller if they are highly correlated.

A ladar signal simulator was developed to synthesize stochastic heterodyne signals. This signal simulator was used to corroborate the theory developed herein and as a source of synthetic signals for a ladar tracker simulator. The track simulator was used to demonstrate closed-loop angle/angle/range/Doppler tracking.

## ACKNOWLEDGEMENTS

This work was conducted under a Lockheed Martin IRAD program. The authors would like to thank Dr. Sammy Henderson for his support of this effort.

## REFERENCES

- 1 R.G. Frehlich and M. Kavaya, *App. Opt.* 30, 1991.
- 2 Degnan and Klein, *App. Opt.*, 13, 1974
- 3 Shapiro, *App. Opt.*, 20, 1981
- 4 Skolnik, *Radar Handbook*, 1970
- 5 J. W. Goodman, *Statistical Optics*, Eqs. 2.8-21 and 2.8-22, John Wiley and Sons, 1985.